

# Amorphous/nanocrystalline silicon biosensor for the specific identification of unamplified nucleic acid sequences using gold nanoparticle probes

Rodrigo Martins<sup>a)</sup>

CENIMAT, Faculdade Ciências e Tecnologia, Departamento de Ciência dos Materiais, Universidade Nova de Lisboa-CEMOP-UNINOVA, 2829-516 Caparica, Portugal

Pedro Baptista

CIGMH/SABT, Faculdade Ciências e Tecnologia, Universidade Nova de Lisboa, 2829-516 Caparica, Portugal

Leandro Raniero

CENIMAT, Faculdade Ciências e Tecnologia, Departamento de Ciência dos Materiais, Universidade Nova de Lisboa-CEMOP-UNINOVA, 2829-516 Caparica, Portugal and Divisão de Materiais, Instituto Nacional de Metrologia, Normalização e Qualidade Industrial, Av. N<sup>a</sup> S<sup>ra</sup> das Graças, 50 Prédop 3, Dimci/Dimat, Xerém, 25250-020 Rio de Janeiro, Brasil

Gonçalo Doria

CIGMH/SABT, Faculdade Ciências e Tecnologia, Universidade Nova de Lisboa, 2829-516 Caparica, Portugal

Leonardo Silva

CENIMAT, Faculdade Ciências e Tecnologia, Departamento de Ciência dos Materiais, Universidade Nova de Lisboa-CEMOP-UNINOVA, 2829-516 Caparica, Portugal

Ricardo Franco

REQUIMTE, Faculdade Ciências e Tecnologia, Departamento de Química, Universidade Nova de Lisboa, 2829-516 Caparica, Portugal

Elvira Fortunato

CENIMAT, Faculdade Ciências e Tecnologia, Departamento de Ciência dos Materiais, Universidade Nova de Lisboa-CEMOP-UNINOVA, 2829-516 Caparica, Portugal

(Received 19 September 2006; accepted 7 December 2006; published online 12 January 2007)

Amorphous/nanocrystalline silicon *p-i-n* devices fabricated on micromachined glass substrates are integrated with oligonucleotide-derivatized gold nanoparticles for a colorimetric detection method. The method enables the specific detection and quantification of unamplified nucleic acid sequences (DNA and RNA) without the need to functionalize the glass surface, allowing for resolution of single nucleotide differences between DNA and RNA sequences—single nucleotide polymorphism and mutation detection. The detector's substrate is glass and the sample is directly applied on the back side of the biosensor, ensuring a direct optical coupling of the assays with a concomitant maximum photon capture and the possibility to reuse the sensor. © 2007 American Institute of Physics. [DOI: [10.1063/1.2431449](https://doi.org/10.1063/1.2431449)]

The use of nanotechnology based systems has boosted the potential applications in clinical diagnostics. This is the case of metal nanoparticles whose surface and geometry can be tailored to selectively bind a subset of biomarkers, either for direct detection and characterization or to capture the target molecules for a later study. Many available techniques are based on colorimetric measurements of the optical properties of the nanoparticles in solution (position change of the plasmon band) before and after binding to the target molecule.<sup>1</sup> Most applications of these nanoparticle-based systems have been largely focused on unamplified nucleic acid sequences (DNA and RNA) or protein-functionalized gold (Au) nanoparticles used as the target-specific probes.<sup>1–3</sup> In solution, monodisperse Au nanoparticles with sizes of about 20 nm appear red and exhibit a relatively narrow surface plasmon absorption band centered around 525 nm<sup>2</sup>. In contrast, at high salt concentrations the nanoparticles aggregate and the solution turns blue-purple, with a characteristic

redshift to longer wavelengths.<sup>3,4</sup> A solution of nonfunctionalized Au nanoparticles aggregates instantaneously after salt addition, whereas nucleic acid sequences protect Au nanoparticles against aggregation.<sup>4–7</sup>

Our method is based on the optical properties of Au nanoparticles derivatized with the appropriate thiolated oligonucleotides of 25–30 bp (base pair), herein known as Au nanoprobes.<sup>7,8</sup> The presence of a fully complementary DNA or RNA sequence as target stabilizes the Au nanoprobes and the solution maintains the red color despite the increase of salt concentration. However, the presence of noncomplementary targets (i.e., DNA or RNA sequences that do not hybridize specifically with the probe) does not prevent particle aggregation and, thus, the solution turns purple.

Detection schemes using chip-based hybridization have been the target of many research groups worldwide. The known electronic detection methods are based on light measurements in photonic structures,<sup>9</sup> complementary metal oxide semiconductor photodetector arrays,<sup>10</sup> or GaAs sensors.<sup>11</sup> All these systems are based on the previous functionalization

<sup>a)</sup>Electronic mail: rm@uninova.pt

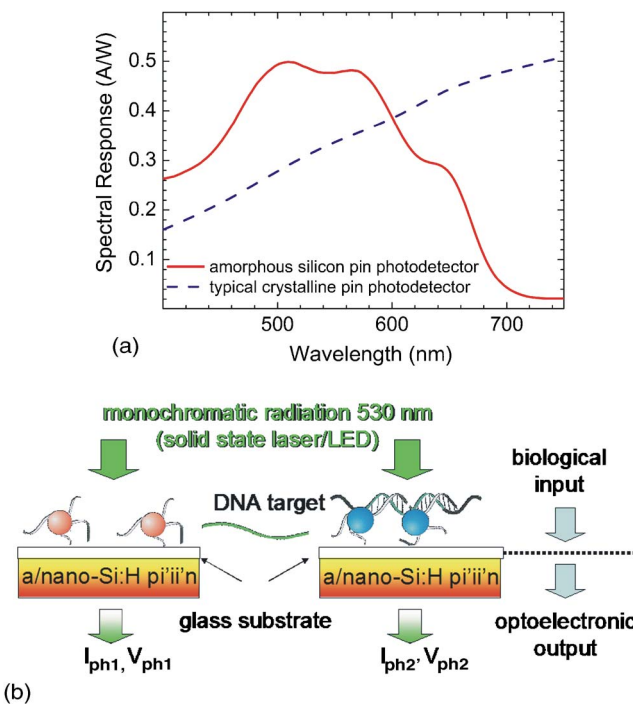


FIG. 1. (Color online) (a) Spectral response of the amorphous/nanocrystalline Si sensor. It is also shown the spectral response due to a crystalline device; (b) schematic of the detection platform used.

of the device sensing element, preventing its reuse in further detection assays.<sup>12</sup>

In this work we present a simple and inexpensive system that integrates the nanoparticle colorimetric detection method and a light sensitive amorphous/nanocrystalline silicon *pi'ii'n* biosensor. The sensors were produced by plasma enhanced chemical vapor deposition on glass substrates using an exciting frequency of 27.12 MHz.<sup>13</sup> The back side of the glass substrate was previously micromachined (3 mm in diameter) to allow deposition of the biological sample. This will ensure a direct optical coupling of the assays to the sensor with concomitant maximum photon capture. Furthermore, this strategy allows for a 90% reduction in the amount of sample solution needed for each analysis when compared with conventional techniques.<sup>1-6</sup>

The different layers of the sensor and their thicknesses are tailored so as to control the spectral response band with an optimal response peak within the 500–650 nm range [see Fig. 1(a)]. It should be noted that the maximum spectral response (0.5 A/W) is attained at around 530 nm, also the maximum absorbance for the Au nanoprobes. The *p*- and *n*-doped layers have conductivities of  $10^{-5}$  and  $10^{-1} (\Omega \text{ cm})^{-1}$  and thicknesses between 20 and 40 nm, respectively.<sup>13</sup> The *i*-sensitive layer was deposited close to the transition region from amorphous to microcrystalline silicon, leading to the improvement of its short to medium range order.<sup>14</sup> The *i* layer has a responsivity above  $10^6$ , for the light intensity used and a thickness of about 300–500 nm. The buffer layers (*i'*) are less than 10 nm thick and constituted by silicon nanocrystals with sizes tailored to match the band gap of the adjacent layers and to allow the proper bandwidth spectral response. The sensor dark current is of about 50 pA when reverse biased with -1 V. The light source used is a solid state laser with a power intensity of 0.5 mW and a wavelength of 530 nm.

Downloaded 29 Jan 2007 to 193.136.125.97. Redistribution subject to AIP license or copyright, see <http://apl.aip.org/apl/copyright.jsp>

To evaluate the performances of this system several assays were made using two sets of experiments: (a) different concentrations of Au nanoprobes alone before and after salt addition, to evaluate the response and sensitivity of the sensor; and (b) Au nanoprobes previously hybridized with a complementary DNA sequence (positive, POS) or non-complementary DNA sequence (negative, NEG). The assay solutions containing the Au nanoprobes and target nucleic acid sequence (previously purified and characterized DNA sample) were prepared by mixing various concentrations of the appropriate target with the Au-nanoprobe solution. After 5 min of denaturation at 95 °C, the mixtures were allowed to stand for 15 min, and NaCl was added to a final concentration of 2M. A reference sample (BLANK) was also prepared exactly in the same conditions as above but now replacing the sample DNA for an equivalent volume of 10 mM phosphate buffer. The sample solution was then placed on the sensor [see Fig. 1(b)] and the measurements performed by illuminating the sample solution with the laser with a spot size equal to that of the sensor. To eliminate the influence of the backlight illumination, the light was pulsed at 130 Hz, without using any passband light filter. The light goes through the glass substrate and it is absorbed by the sensor, generating an electrical signal (current) that is detected by an electrometer. In the present case we used a lock-in amplifier with a V/A conversion of  $10^6$ . As the sensor works in the photovoltage mode,<sup>15</sup> the laser light serves simultaneously to infer the absorption in biological sample as well as to activate the sensor. The detection response  $R_{\text{det}}$  is defined as the difference between the reference value  $R_{\text{ref}}$  and the values obtained in presence of sample solution,  $R_{\text{DNA}}$ ,

$$R_{\text{det}} = R_{\text{ref}} - R_{\text{DNA}}, \quad (1)$$

$R_{\text{ref}} (>R_{\text{DNA}})$  is the value of the current measured by shining light directly on the sensor. To determine the reliability of the process we used decreasing Au-nanoprobe concentrations ranging from 7.6 to 1.8 nM [inset, Fig. 2(a)]. The data show a linear behavior between  $R_{\text{det}}$  and the probe concentration. Concentrations of Au nanoprobe under 1 nM generate  $R_{\text{det}} \approx 0$ , meaning that  $R_{\text{ref}}=R_{\text{DNA}}$  and so the minimum detection limit imposed by the signal to noise ratio is reached.

We then used this device to directly detect the presence of DNA sequences from *Mycobacterium tuberculosis*, the etiologic agent for tuberculosis. A purified fragment of rpo “beta” gene (RNA polymerase beta), allowing for detection of *M. tuberculosis*, was used as fully complementary target.<sup>8</sup> Samples were prepared as described above but the Au-nanoprobe concentration was kept constant at 2.5 nM. Measurements were made with the reference (blank); noncomplementary DNA (NEG) and complementary DNA (POS). Two fragments of different lengths were used, one with 200 bp and another with 400 bp—POSA and POSB, respectively.

Figure 2(a) shows that despite all sample solutions absorbing the incident radiation, a clear difference between complementary (POS) and noncomplementary (NEG) is noticeable. The  $R_{\text{ref}}$  values for the BLANK mean that the solution prepared absorbs some light that could be related to the so-called drop effect of the sample solution (changes in the refractive index between the solution and the air and to the convex geometry of the drop). To eliminate this effect  $R_{\text{ref}}$  should be measured with the BLANK. The performed measurements were consistent and reproducible and were simultaneously confirmed by UV/visible spectroscopic measure-

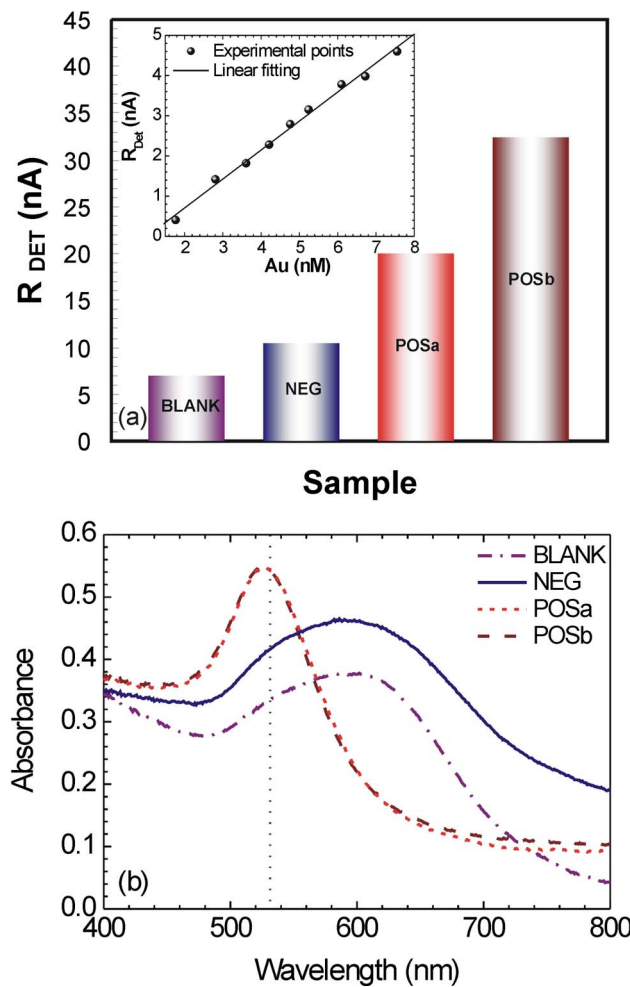


FIG. 2. (Color online) (a) Output response signal of the biosensor for different samples. Complementary DNA target: POSa and POSb (red and wine color, respectively); noncomplementary DNA target: NEG (navy color) and BLANK (purple color). The inset shows the sensor response as function of the Au-nanoprobe concentration, with a correlation better than 0.997 for the linear fitting; (b) absorbance spectra of the same set of samples analyzed: short dash red line for POSa, dashed wine line for POSb, solid navy line for NEG, and dot purple line for BLANK.

ments [Fig. 2(b)]. However, the described sensor requires ten times smaller sample volumes and has a higher sensitivity than the conventional spectrophotometer based assays. This way, it was possible to specifically detect less than 1 pM target DNA. This considerable increase in sensitivity is depicted in Fig. 2(a), where longer DNA target fragments produce higher output signals (POSb). The subtle effect on Au-nanoprobe stability of the target DNA fragment length can be detected by the described sensor, while impossible to ascertain via conventional spectrophotometry [see POSa and POSb in Figs. 2(a) and 2(b)]. Longer target DNA fragments

are known to cause stronger repulsion of the nanoparticles, thus increasing their stability in solution.<sup>6</sup> This effect can be used towards development of single base mismatch detection for single nucleotide polymorphism analysis and mutation characterization.

The described system presents several advantages when compared with more conventional approaches: (i) no need to functionalize the glass surface with probe DNA; (ii) the substrate is glass, allowing for the sample to be directly applied on the back side of the nanostructured sensor ensuring maximum photon capture; (iii) less than 1 pM of target can be detected without any enhancement steps. The described system combines two technologies—gold nanoparticle based DNA detection and optical sensors based on thin film technology—leading to significant cost and time savings in DNA assays, allowing for molecular diagnostics at point of care, without compromising specificity and sensitivity (e.g., doctor's practice, laboratory bench, in the field, where a display can be powered with a 1.5 V battery).

This work was supported by FCT/MCTES through pluriannual contract programs with CENIMAT, REQUIMTE, and CIGMH, Grant POCTI/QUI/45141/2002, fellowship SFRH/BD/6888/2001 and F. C. Gulbenkian through project with Ref 76436.

- <sup>1</sup>J. J. Storhoff, D. A. Lucas, V. Garimella, Y. P. Bao, and U. R. Muller, *Nat. Biotechnol.* **22**, 883 (2004).
- <sup>2</sup>C. A. Mirkin, R. L. Letsinger, R. C. Mucic, and J. J. Storhoff, *Nature (London)* **38**, 607 (1996).
- <sup>3</sup>J. Nam, S. I. Stoeva, and C. A. Mirkin, *J. Am. Chem. Soc.* **126**, 5932 (2004).
- <sup>4</sup>K. Sato, K. Hosokawa, and M. Maeda, *J. Am. Chem. Soc.* **125**, 8102 (2003).
- <sup>5</sup>M. Huber, T. Wei, U. R. Müller, P. A. Lefebvre, S. S. Marla, and Y. P. Bao, *Nucleic Acids Res.* **32**, 137(E) (2004).
- <sup>6</sup>M. P. Sandström, M. Boncheva, and B. Kerman, *Langmuir* **19**, 7537 (2003).
- <sup>7</sup>P. Baptista, G. Doria, D. Henrique, E. Pereira, and R. Franco, *J. Biotechnol.* **119**, 111 (2005).
- <sup>8</sup>P. V. Baptista, M. Koziol-Montewka, J. Paluch-Oles, G. Doria, and R. Franco, *Clin. Chem.* **52**, 1433 (2006).
- <sup>9</sup>Bradley Schmidt, V. Almeida, C. Manolatou, Stefan Preble, and M. Lipson, *Appl. Phys. Lett.* **85**, 4854 (2004).
- <sup>10</sup>A. Frey, F. Hofmann, R. Peters, B. Holzapfl, M. Schienle, C. Paulus, P. Schindler-Bauer, D. Kuhlmeier, J. Krause, G. Eckstein, and R. Thewes, *Microelectron. Reliab.* **42**, 1801 (2002).
- <sup>11</sup>Y. Paltiel, A. Haroni, U. Banin, O. Neuman, and R. Naaman, *Appl. Phys. Lett.* **89**, 033108 (2006).
- <sup>12</sup>F. Fixe, R. Cabeça, V. Chu, D. M. F. Prazeres, G. N. M. Ferreira, and J. P. Conde, *Appl. Phys. Lett.* **83**, 1465 (2003).
- <sup>13</sup>L. Raniero, I. Ferreira, L. Pereira, H. Águas, E. Fortunato, and R. Martins, *J. Non-Cryst. Solids* **352**, 1945 (2006).
- <sup>14</sup>R. Martins, H. Águas, I. Ferreira, E. Fortunato, S. Lebib, P. Roca i Cabarcos, and L. Guimarães, *Adv. Mater. (Weinheim, Ger.)* **9**, 333 (2003).
- <sup>15</sup>E. Fortunato, L. Pereira, H. Águas, I. Ferreira, and R. Martins, *Proc. IEEE* **93**, 1281 (2005).